General Disclaimer

One or more of the Following Statements may affect this Document

- This document has been reproduced from the best copy furnished by the organizational source. It is being released in the interest of making available as much information as possible.

- This document may contain data, which exceeds the sheet parameters. It was furnished in this condition by the organizational source and is the best copy available.

- This document may contain tone-on-tone or color graphs, charts and/or pictures, which have been reproduced in black and white.

- This document is paginated as submitted by the original source.

- Portions of this document are not fully legible due to the historical nature of some of the material. However, it is the best reproduction available from the original submission.

TERMINATION REPORT

TO THE

LUNAR AND PLANETARY INSTITUTE

Houston Jep

NASW · 3389

W.J. RUSSELL

AUGUST 10, 1984

I. INTRODUCTION:

This paper serves as a termination report to the Lunar and Planetary Institute. It documents the research I was involved while working as a research assistant to Dr. Gary Lofgren (in the experimental Petlab at the Johnson Space Center.) Our work involved the dymanic crystallization of silicate melts and focused on the effects of heterogeneous nucleation on crystallization. The term dynamic crystallization is used as opposed to equilibrium crystallization indicating changing conditions during crystallization (in this case temperature changes). The term heterogenous nucleation refers to nucleation on a foreign ·substrate present in the liquid which reduces the activation barrier to nucleation by reducing the surface free energy (Lofgren, 1983). We are primarily concerned with nucleation occuring within the liquid and not on the container walls. This is termed internal nucleation and most likely occurs on impurity particles or unmelted remnants.

The materials used in this study were of chondrule composition. Melt temperature and cooling rate were varied systematically for the different compositions. The purpose of these studies is to duplicate the disequilibrium features displayed by minerals in rocks and to better understand how these features and ultimately the rocks form.

Previous work by Hewins et al (1981) on a similar composition material demonstrated a relationship between the size and composition of the dendrites in radial pyroxene chondrules and cooling rate. Hewins was attempting to reproduce the textures of chondrules in Manych (LL3 chondrite), but reproduced only those with a radial texture. Hewins suggested a broader range of cooling rates be used and the effects of heterogeneous nucleation be studied.

Tsuchiyama et al, (1980) experimented with three chondrule compositions by using a single melt temperature and various cooling rates. They recognized the importance of nucleation temperature but suggested that because nucleation temperature is in part affected by cooling rate it would be best to restrict the study to a single melt temperature. Although these studies produced porphyritic, barred and radial textures, the textures were each restricted to an individual composition. They concluded that cooling was subordinate to composition in controlling texture.

In a later study Tsuchiyama and Nagahara (1981) investigated the effect of precooling thermal history coupled with a variety of cooling rates. Cooling rates from 800 to 5.3C/hr were used for both subliquidus and super-liquidus melts. Their study produced a wider variety of textures than the previously mentioned study, illustrating the effect relict crystals have an texture.

This present study examines a broader range of cooling rates and systematically examines six starting material covering a range of chondrule compositions both with and without minerals present. Two abstracts have been published previous to this (Lofgren et al, 1984) documenting preliminary results of this study.

II. Experimental Apparatus

Two types of gas mixing furnaces were used in these experiments. These are known as the Deltech and Astrofurance. The most significant difference between these two types is the temperature range capabilities. The Deltech can be used at temperatures up to $1575^{O}C$ while the astrofurance can be used at temperatures in excess of $1700^{O}C$. At these extreme temperatures, however, the muffle tube in the astro furance is removed and an inert atmosphere such as argon must be used instead of the regular buffering gases.

The furances operate under atmospheric pressures and use a mixture of carbon monoxide and carbon dioxide as gaseous buffers. This mixture of gases react with one another at high temperature to release or consume oxygen. This permits oxygen fugacity to be varied independent of temperature (Nafziger et al, 1971). This buffering is based on the dissociation of CO_2 at high temperatures ie. $CO_2 = CO + 1\backslash2$

O_2. Hence the oxidation or reduction conditions are controlled by the relative abundances of CO_2 and CO.

The oxygen fugacity is measured directly using an electrolyte ceramic cell in the furance (Fig. 1). Pure oxygen is pumped through the interior of the cell while the controlled furnace atmosphere circulates about the exterior of the cell. The net reaction at the cell is $O_2 + 4e^- = 2O^{-2}$. This ion exchange creates a voltage across the cell wall which is a function of the fO_2 on both the inside and the outside of the cell and the furnace temperature. This voltage is easily monitored and the fO_2 in the furnace can be calculated as

$$\log fO_2 = \frac{2.0159}{T} E;$$

provided pure oxygen at 1 bar is used as the reference gas (Williams and Mullins, 1981). Hence by monitoring this voltage the fO_2 in the furnace can be accurately monitored. A temperature vs. $\log fO_2$ illustrates $CO-CO_2$ buffer curves in figure 2. For these experiments the NNO buffer curve was used to calibrate the electrolyte cells. NiO pellets were suspended in the hot spot of the furnace in an oxidizing atmosphere (ie. above the NNO buffer curve, see fig. 2). The CO/CO_2 gas ratio was increased systematically and the pellet was removed periodically while monitoring the millivoltage generated by the cell. When the NiO is reduced
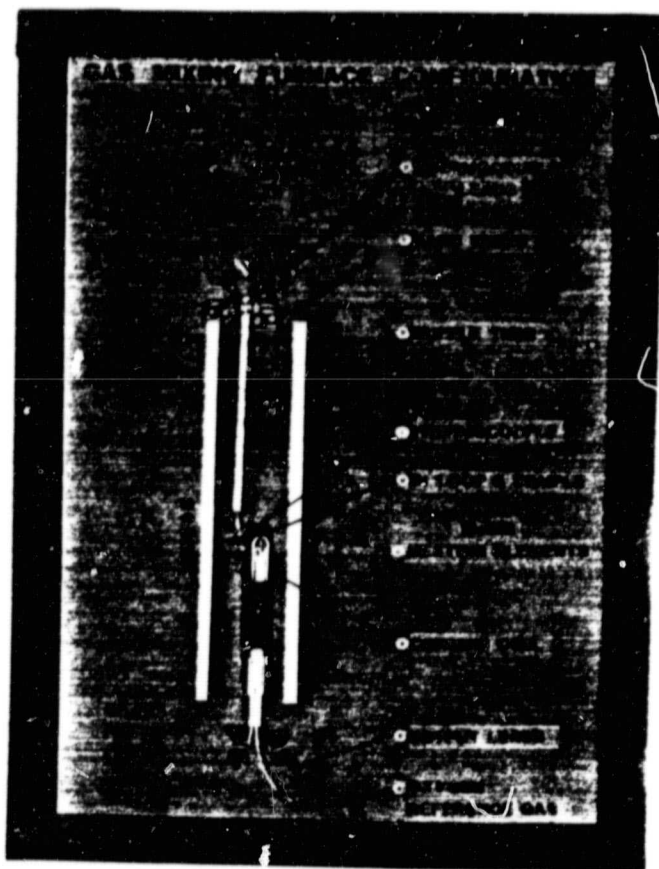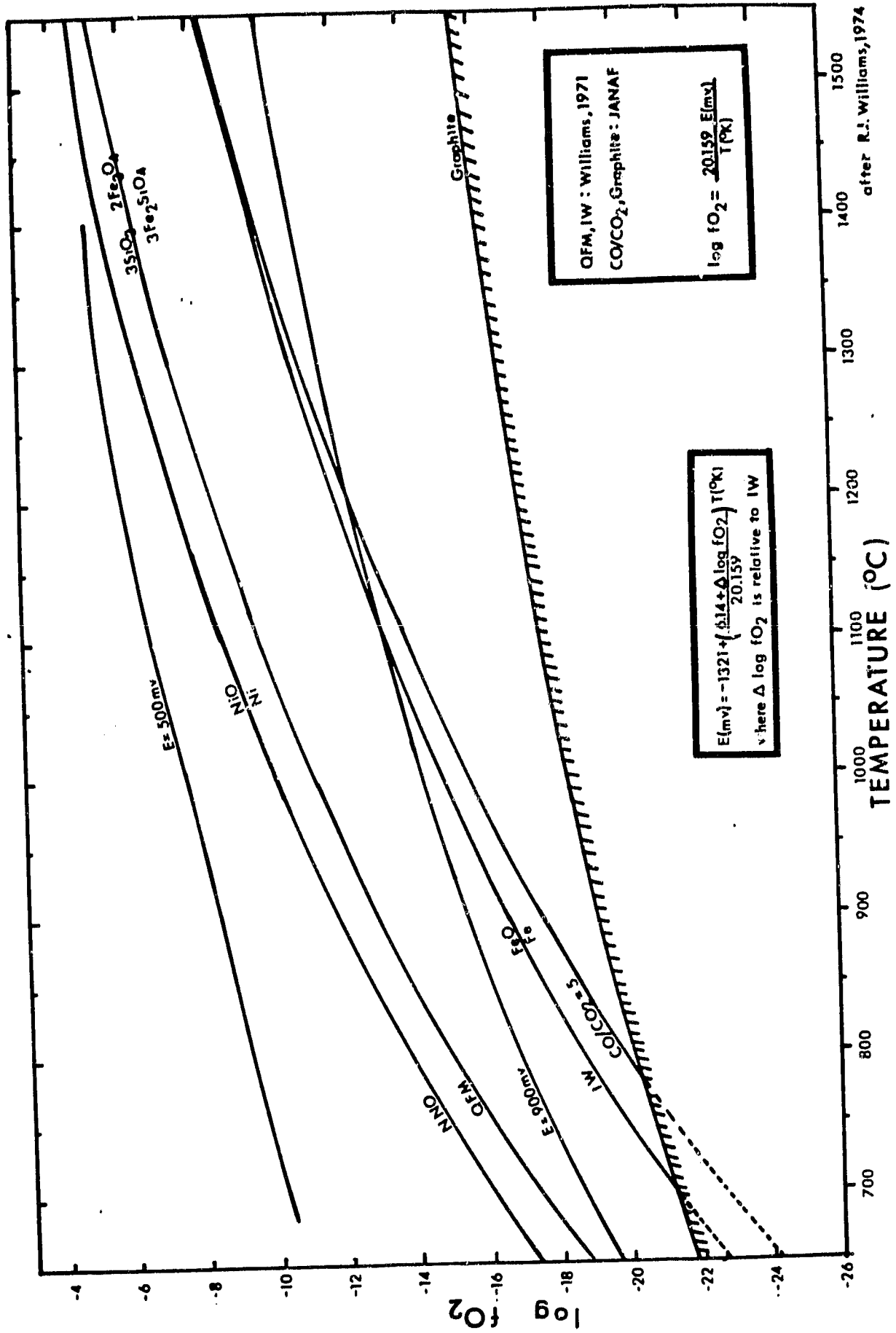
FIG.1. Furnace Configuration

FIG.2. Buffer Curves

after R.I. Williams, 1974

QFM, IW : Williams, 1971
CO/CO_2, Graphite : JANAF

$$\log fO_2 = \frac{20.159 \ E(mv)}{T(^\circ K)}$$

$$E(mv) = -1321 + \left(\frac{6.14 + \Delta \log fO_2}{20.159}\right) T(^\circ K)$$

v here $\Delta \log fO_2$ is relative to IW

TEMPERATURE (°C)

log fO_2

to Ni (pellet turns from green to grey) the process can be reversed. Approximately 15 minutes is required for the reduction or oxidation process. After calibration fO_2 values are accurate to +/- 0.2 log units.

Temperature is monitored using Pt/Rh thermocouples. For experiments utilizing temperatures in excess of $1300^{\circ}C$ type B (Pt6Rh-Pt30Rh) thermocouples are used. For lower temperatures type S thermocouples are used (Pt-Pt10Rh). Thermocouples are calibrated regularly against the melting point of various metals depending on the temperature range of the experiments. Gold (1063° C), nickel ($1453^{\circ}C$), and palladium ($1552^{\circ}C$) are used for this purpose. Temperatures reported are believed accurate to +/- $5^{\circ}C$.

A controller thermocouple is also built into the furnaces. The presence of the two thermocouples together makes it possible to have temperature programming for non-isothermal experiments. The details of this device are discussed thoroughly by William and Mullins (1981). Briefly the furnace temperature is set using the controller and built in thermocouple. An additional millivoltage is then added using the programmer resulting in a higher temperature. This additional millivoltage can then be subtracted at regular increments resulting in a steady decrease in temperature. Furthermore, initial delay setting can be used to create relatively complex programmed cooling (or melt) histories.

III. EXPERIMENTAL PROCEDURE.

Three starting compositions were prepared which attempted
to duplicate the bulk chemistry of chondrules known as
porphyritic pyroxene, radial pyroxene and porphyritic
olivine. (As reported by McSween, 1977; Dodd, 1978; Kimura
and Yagi, 1980; Lux et al, 1981. For each composition two
different starting materials were prepared, one from a fused
mixture of oxides and the other from a mixture of minerals.
The oxide and mineral mixtures for each composition are very
similar, but not identical. The objective was to obtain a
glassy or near glassy (the glass contains some fine olivine
dendrites) and a totally crystalline (with a variety of
minerals) starting material. The minerals used are olivine,
enstatite, bytownite, albite and magnetite. Both types of
starting material were finely ground. See Table 1 and Figure
3 for compositions.

Experimental run procedures are similar to those reported
by Lofgren (1983). Platinum wire loops were electro-plated
with iron (25 wt.% for radial pyroxene and 12 wt.% for
porphyritic pyroxene and porphyritic olivine) to minimize
the loss of iron from the sample. Electron microprobe
analysis of experimental glass charges indicates that iron
loss is minimized for runs within the time frame of these
experiments. Losses which do occur vary directly with melt
temperature and melt time. Some short runs (3 hr.) show

Table 1. Starting compositions

	PORPHRITIC OLIVINE		PORPHRITIC PYROXENE		RADIAL PYROXENE	
	CH-1*	PO**	CH-2*	PP**	CH-3*	RP**
SIO2	48.67	50.20	55.17	56.51	53.32	54.75
TIO2	0.20	0.01	0.11	0.04	0.07	0.03
AL2O3	4.03	6.41	2.81	4.47	1.87	3.71
CR2O3	0.43	0.01	0.56	0.00	0.31	0.01
FEO	10.97	9.62	9.63	8.03	17.49	16.24
MNO	0.31	0.06	0.33	0.04	0.33	0.04
MGO	32.70	31.34	28.92	27.64	24.23	21.91
CAO	1.86	2.65	1.45	1.85	1.20	1.20
NA2O	0.11	0.15	0.65	1.03	0.52	0.74
K2O	0.00	N.A.	0.05	0.09	0.05	0.14
TOTAL	99.28	100.45	99.70	99.67	99.39	98.95

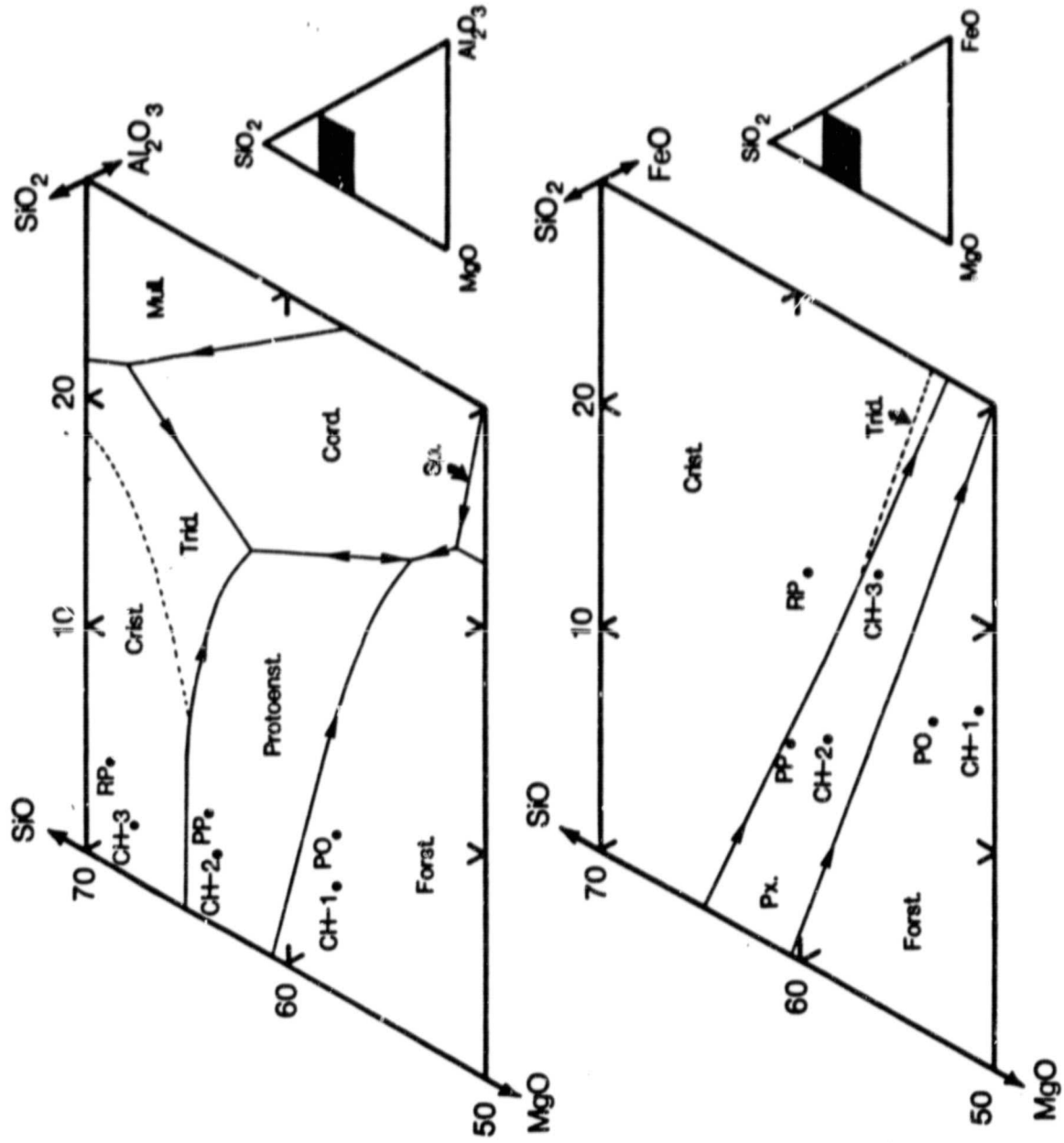*   Oxide mixture

** Mineral mixture

FIG.3. Ternary plot showing six starting compositions.

slight increases in Fe content of the sample suggesting that the Fe plating initially diffuses into the silicate melt. Longer runs show slight decreases in Fe content indicating that the ultimate direction of iron diffusion is into the Pt loop. Iron loss is also a function of the ratio between the size of the sample and the surface area of platinum exposed to the sample. For this reason starting material was weighted out into 75 mg. samples and a constant loop size was used for all runs. All experiments were run in a mixture of CO and CO_2 gases producing an oxygen fugacity approximately 0.5 log units below the Iron-Wustite buffer curve. All charges were melted for 17 hours prior to cooling (except PO and CH-1 which were melted for 2 hours). Charges were cooled to sub-solidus temperatures (except in the case of $65^{\circ}C$/sec.) before being quenched in air.

Experimental charges are mounted in epoxy and cut into approximately six 500 micron thick slices. These slices are then used to make doubly polished thin sections. These thin sections are used for petrographic study and microprobe analysis. Probe analyses were done on the JSC Kameca electron microprobe using an accelerating potential of 15 KV. and a beam current of 30 na (20 na for glasses). Natural minerals were used as standards. The Kameca ZAF reduction scheme was used for results shown here.

IV. EXPERIMENTAL APPROACH

For each of the six starting materials a series of
experiments were designed to incorprate a variety of melt
temperatures and a variety of cooling histories. Melt
temperatures varied 'from sub-liquidus to super-liquidus with
approximately 15-20°C difference between experiments and a
range of 50°C except in the case of RP which has a total
range of 25°C. This variation in melt temperature was used
to vary the amount of heterogeneous nuclei in the charge
prior to cooling. Four different cooling rates were used
for each melt temperature. They are: Quench (65°C/sec.);
Furnace shut off,(FSO) (1800-2500°C/hr.); 100°C/hr. and
5°C/hr. ' A matrix of melt temperature vs. cooling rate was
constructed to illustrate the experimental results. They
are shown in Fig. 4.

V. EXPERIMENTAL RESULTS

Results discussed here concentrate on porphyritic
pyroxene and radial pyroxene compositions. Experiments on
porphyritic olivine compositions are still in progress.

Melting Relations

Phase relations are very difficult to determine
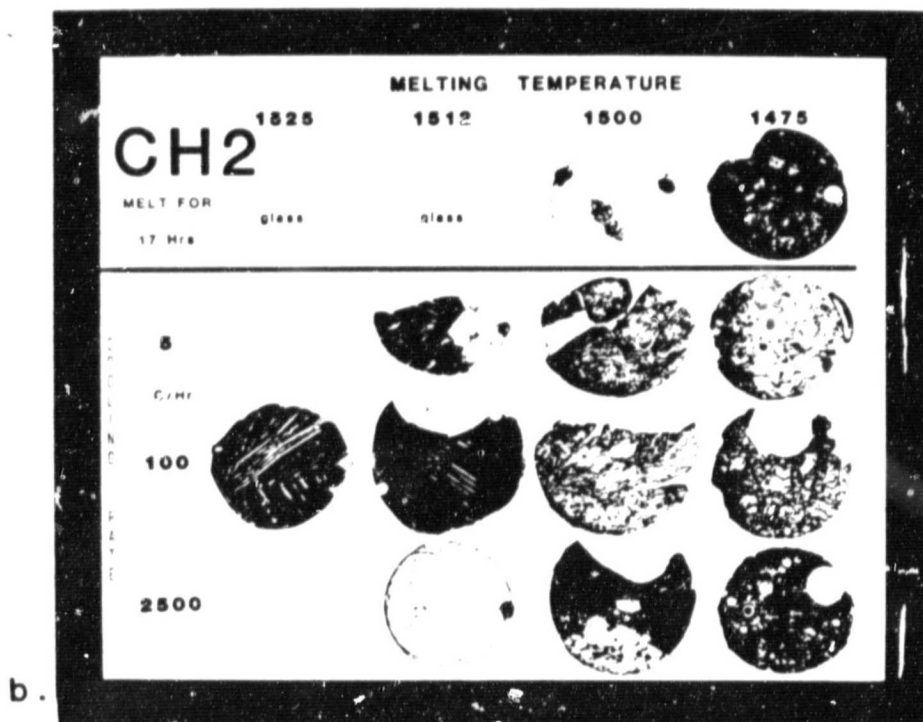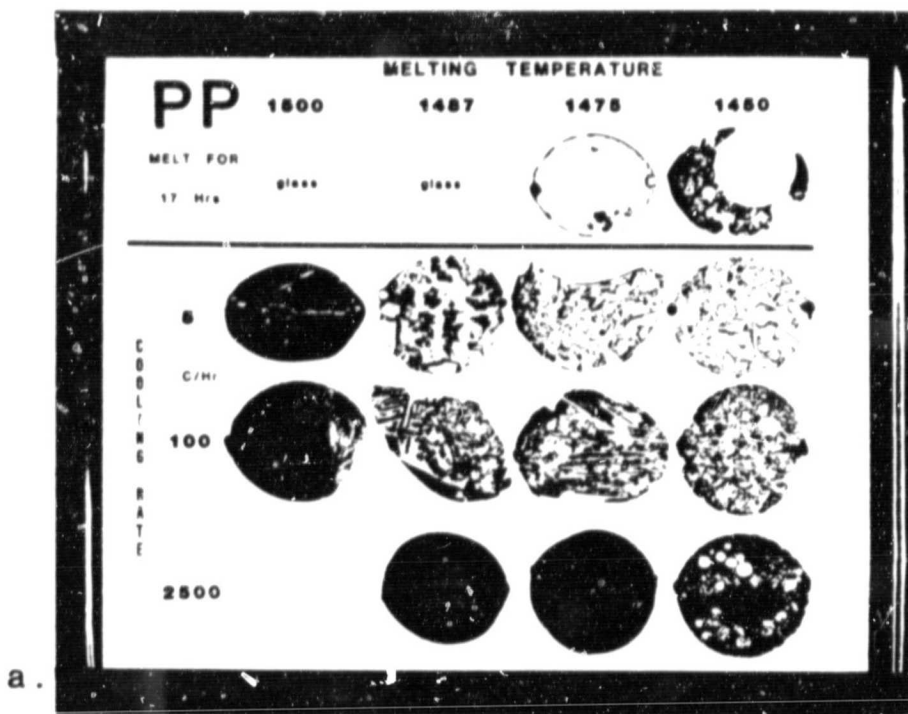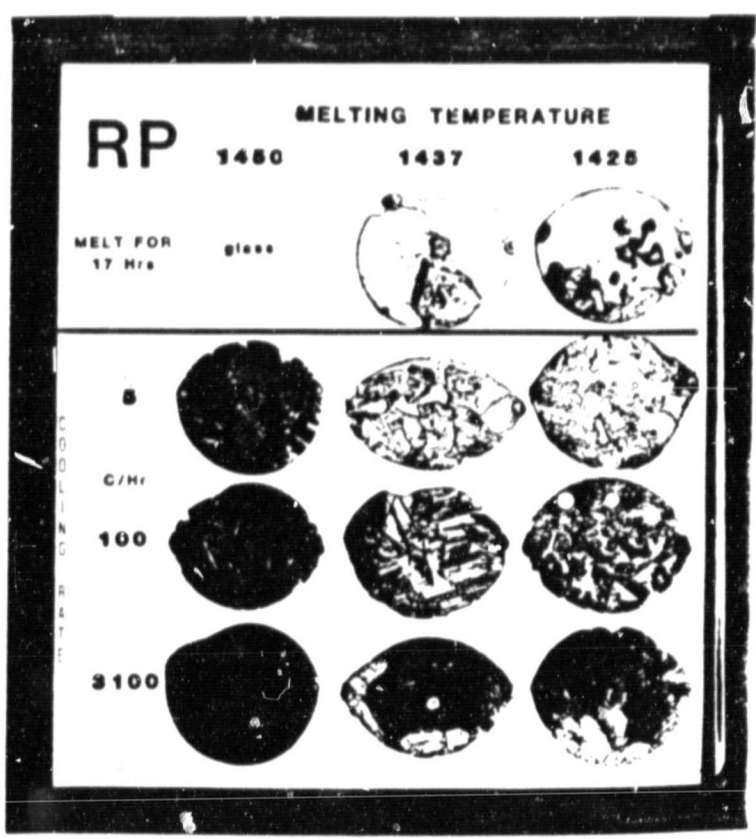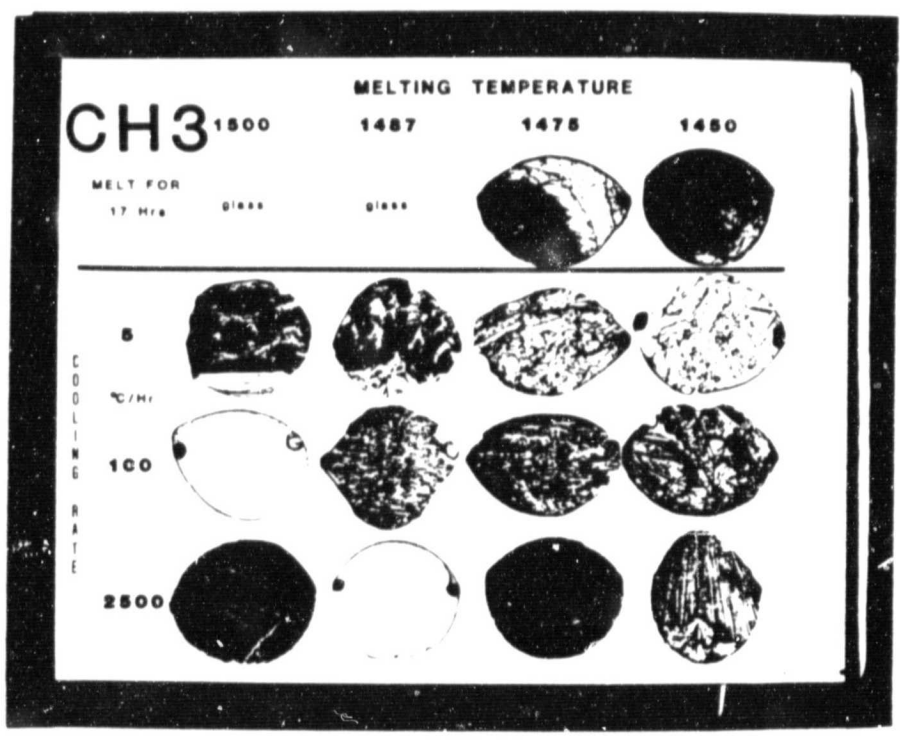accurately because of the inevitable nucleation problems.

FIG. 4.Matrix cooling experiments.(a-e)

c.

d.

CH1

MELTING TEMPERATURE

1600   1585   1570   1550
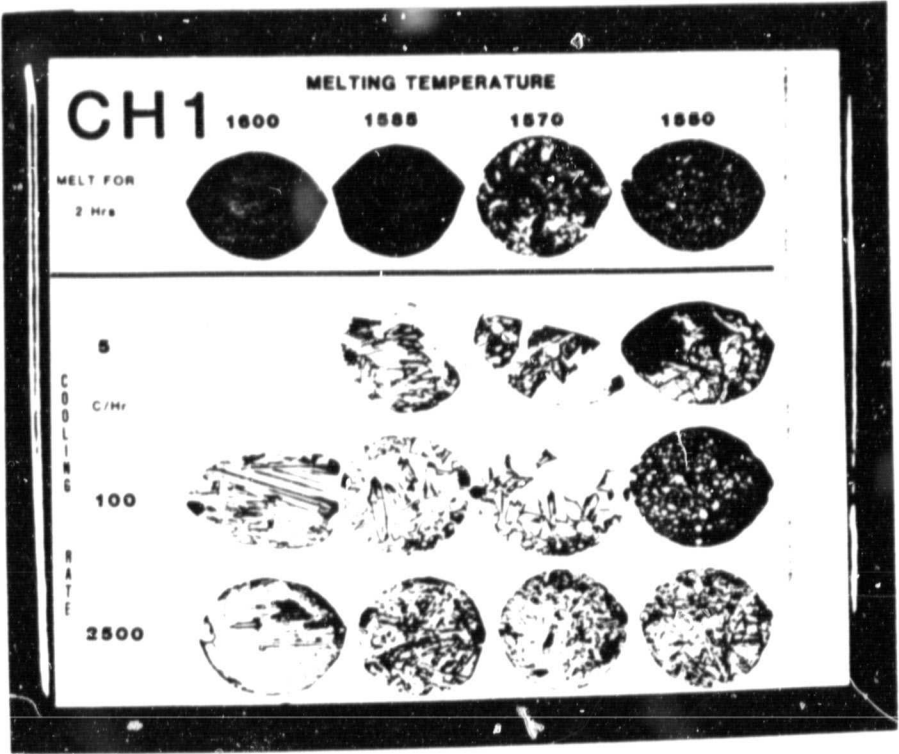
MELT FOR
2 Hrs

5
C/Hr

COOLING RATE

100

2500

e.

For our purposes here, melt relations are more appropriate.
Melt relations were determined by melt experiments.
Crystals up to 3.5 mm. grew during isothermal runs which
were quenched after seventeen hours. Olivine is the
liquidus phase for all compositions. It is however
apparently only metastable in the porphyritic and pyroxene
and radial pyroxene compositions. Charges in which pyroxene
also appears, contain olivine crystals that are generally
rounded and are commonly enclosed by pyroxene. This
indicates partial resorption of the liquidus phase (olivine)
upon crystallization of pyroxene.

The liquidus temperatures for CH-2, PP, CH-3, and RP are
$1500^{o}C$, $1475^{o}C$, $1480^{o}C$, and 1440° $+/-$ $5^{o}C$ respecttively.
The appearance temperature of pyroxene is approximately $15^{o}C$
below the liquidus for the porphyritic pyroxene compositions
(CH-2 and PP). In the case of the radial pyroxene
compositions, the appearance temperature of pyroxene is only
slightly lower than the liquidus temperature.

Tridymite is the only other crystalline phase present.
It appears only in the radial pyroxene compositions as the
last phase to crystallize.

Textures

These experiments produced a wide range of textures
including granular olivine and pyroxene, porphyritic olivine
and pyroxene, radial pyroxene and barred olivine and

pyroxene (Fig 5 and 6). As well, there are an almost infinite number of transitional textures formed, providing a continuous spectrum of textures from granular pyroxene to barred olivine.

The entire textural range is best illustrated by the porphyritic pyroxene compositions (PP and CH2). Compositionally these starting materials are between the porphyritic olivine and radial pyroxene (Fig. 3). End member textures can not be produced using the porphyritic and olivine and radial pyroxene compositions because they can not easily crystallize pyroxene and olivine respectively. All compositions exhibits the same textural trends with respect to variations in melt temperature and cooling rate and consequently only PP and CH2 are described in detail here and results are discussed as a whole as opposed to by individual composition. Summaries of petrographic descriptions are giving in matrix form in tables 2-5.

With the PP composition, subliquidus melt temperatures of 1450°C produce a high density of crystals. Both granular and porphyritic textures are produced. Textures are not completely uniform because of the effects of gravity on crystals. Vesicles are commonly present in zones where small crystals are concentrated. At this temperature both pyroxene and olivine grow during the 17 hour melt period. Olivine appears only as inclusions, pyroxene on the other hand, grows as equant poikilitic crystals. Apparently both
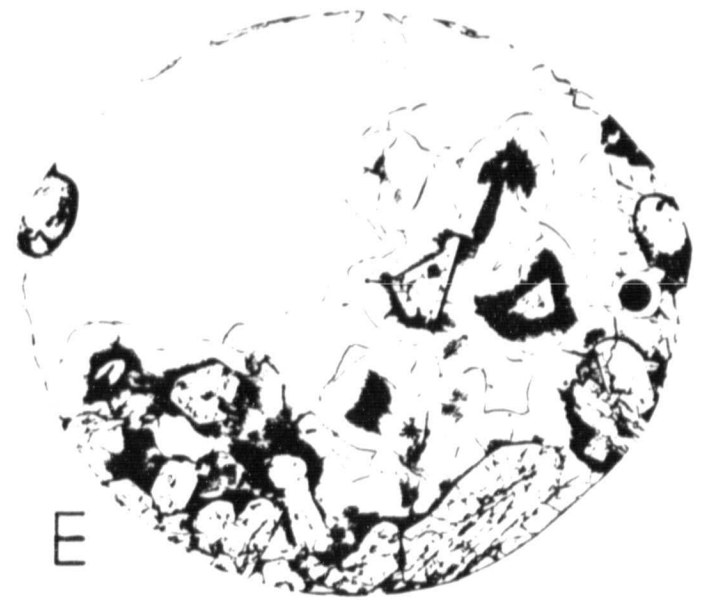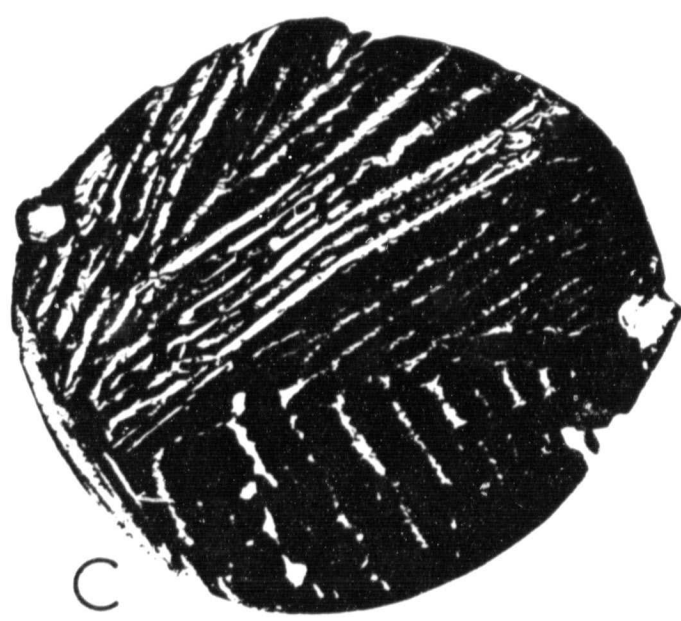
1.0 mm   FIG. 5.

A

B
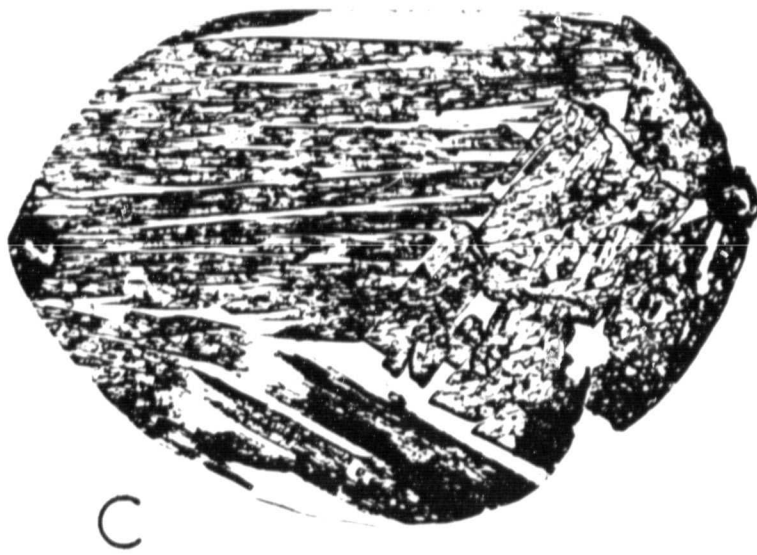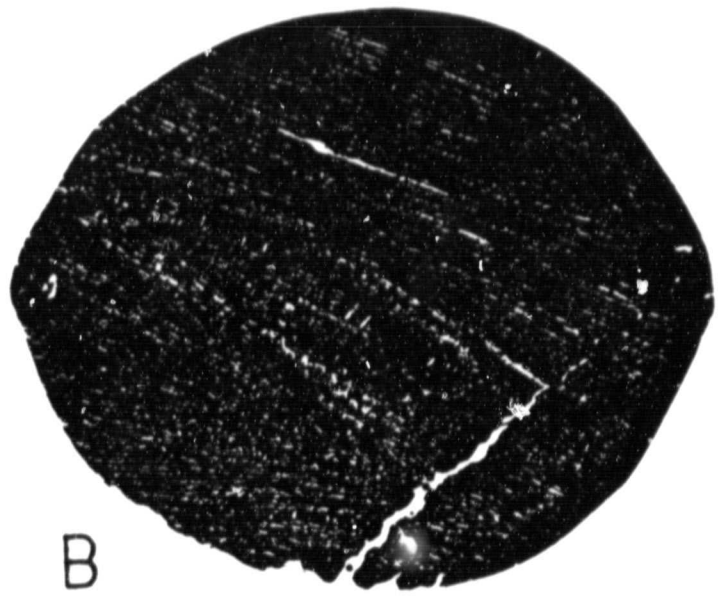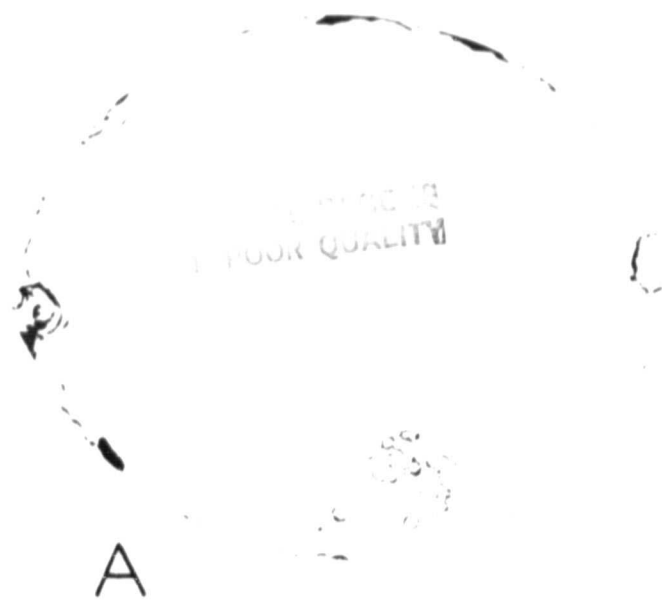
C

D

E

F
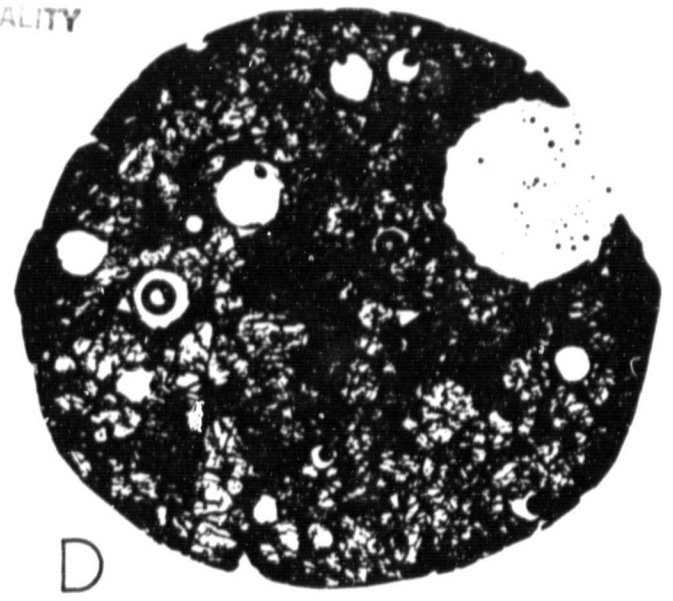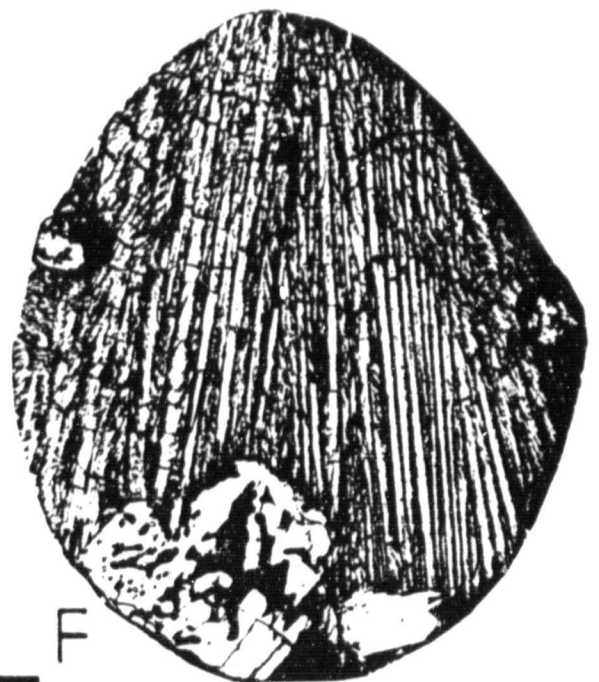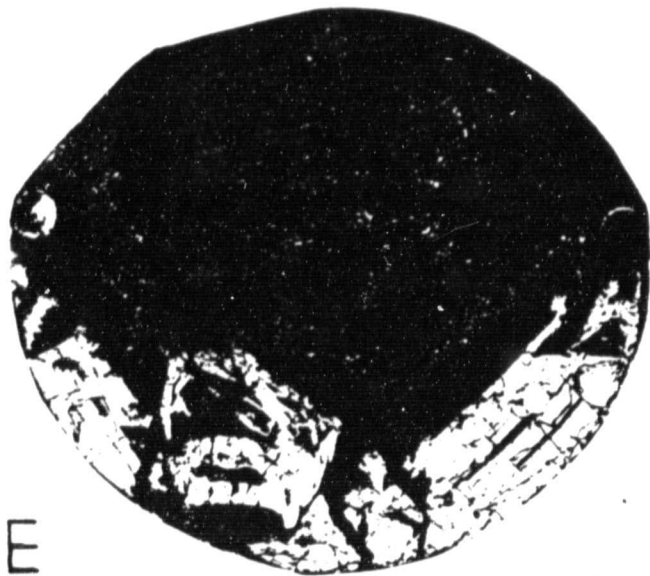
1.0 mm   FIG. 6.

Table 2. PP Matrix

	Melt-1500°C/Quench-1200°C	Melt-1487°C/Quench-1175°C	Melt-1475°C/Quench-1175°C	Melt-1450°C/Quench-1150°C
Quench	GLASS	GLASS	GLASS/PORPHYRITIC OLIVINE -euhedral, equant olivine, settled to bottom have quench overgrowth of spherulitic olivine and opx (?) quench xals	PORPHYRITIC PYROXENE -euhedral, equant, seriate opx, some with olivine incl, some have lamellae -matrix is opx sph and dendrites and glass -vesicles
FSO	-no experiment	RADIAL PYROXENE -uniform, fine, radiate to dend opx	RADIAL PYROXENE -uniform, fine, radiate to dend opx	PORPHYRITIC/GRANULAR PYROXENE -bottom of charge has large, equant, euhedral opx have olivine inclusions in matrix of opx dendrites, -top of charge has nearly equigranular opx and olivine xals -vesicles
100°/hr	RADIAL OLIVINE -fine radiate opx (and olivine?)	GLASS	BARRED PYROXENE -very large, skel to dend opx -might be called barred opx	PORPHYRITIC/GRANULAR PYROXENE -bottom of charge has large, equant to tabular, skel opx xals -top has smaller, equant, euhedral opx xals giving a more equigranular texture -vesicles
5°/hr	BARRED OLIVINE -poorly developed parallel olivine dendrites -matrix is opaque quench xals	PORPHYRITIC OLIVINE -large, tab, sl skel olivine settled to bottom, have dendritic projections -matrix acic to dend opx and olivine, few small, equant euhedral opx, and glass	PORPHYRITIC PYROXENE -three large, euhedral, skel opx with lamellae, some have olivine inclusions -opx dendrites in glass	PORPHYRITIC PYROXENE -large, euhedral, equant opx have lamellae, settled to bottom -top of charge is more densely packed with smaller, equant opx with olivine inclusions -vesicles

Table 3. CH2 Matrix

	Melt-1525°C/Quench-1225°C	Melt-1512°C/Quench-1212°C	Melt-1500°C/Quench-1200°C	Melt-1475°C/Quench-1175°C
Quench	GLASS	GLASS	GLASS/PORPHYRITIC OLIVINE -equant, euhedral olivine clustered in center of the charge enclosed in feathery olivine quench xals	PORPHYRITIC PYROXENE -euhedral, tab to equant, sl skel opx containing numerous, rounded olivine inclusions, some opx have lamellae -dendritic to feathery opx quench xals project or radiate from large opx
5°/hr		PORPHYRITIC OLIVINE -large, skel olivine -matrix fine, radiate and dend opx	PORPHYRITIC PYROXENE -equant, euhedral to subhedral opx with lamallae -some olivine inclusions -matrix is glass (10%)	PORPHYRITIC PYROXENE -equant to sl tab, euhedral to subhedral, sl skel opx, some have lamallae -granular mass of small opx mixed with vesicles at top of charge
100°/hr	BARRED OLIVINE -long, course, dendritic (barred?) olivine -fine, elong, quench xals (olivine?) oriented with larger xals -small areas of glass and fine radiate opx	BARRED OLIVINE -few, elong, skeletal olivine -parallel growth dendritic olivine quench xals -small areas of glass and fine opx dendrites and radiate xals	PORPHYRITIC PYROXENE -euhedral, tab to elong skel to dend opx with lamellae -numerous inclusions of rounded to euhedral olivine in opx at bottom of charge	PORPHYRITIC PYROXENE -equant, euhedral opx, most have lamellae, few have olivine inclusions -glass less than 10% -few vesicles
FSO	-no experiment	GLASS	PORPHYRITIC PYROXENE -large, euhedral opx, most have lamellae -small, rounded olivine inclusions in opx -60% of charge is fiberous opx dendrites and radiate opx	PORPHYRITIC PYROXENE -euhedral to anhedral, equant opx, most have lamellae and some with olivine inclusions -vesicles -less than 5% glass

Table 4. RP Matrix

	Melt-1450°C/Quench-1150°C	Melt-1437°C/Quench-1137°C	Melt-1425°C/Quench-1125°C
Quench	GLASS	PORPHYRITIC PYROXENE -two large, equant, euhedral, skeletal opx, lamellae throughout -spherulitic quench xals surrounding opx xals -approx. 65% glass	PORPHYRITIC PYROXENE -partially settled, euhedral, equant to tab opx, lamellae in most -one twinned opx -two partially rounded opx without lamellae -spherulitic quench xals surrounding larger xals -approx. 35% glass
5°/hr	RADIAL PYROXENE -excentroradial opx fine-grained fibers	PORPHYRITIC PYROXENE -large, euhedral, equant, sl skel opx, some have lamellae -approx. 30% glass -rind of small xals on top surface of charge, SiO_2 mineral (tridymite?)	PORPHYRITIC PYROXENE -large, euhedral, elong, sl skel opx, sparse lamellae in cores, sl zoning -some vesicles -approx. 30% glass
100°/hr	RADIAL PYROXENE -fine and coarse-grained, radiate opx, small angle branches - almost dend	PORPHYRITIC PYROXENE -elong, skel opx, some have lamellae -15% glass present	PORPHYRITIC PYROXENE -elong, tab opx, some have lamellae -smaller xals at top(?) of charge, olivine and opx -approx. 10% glass -vesicles
FSO	RADIAL PYROXENE -very fine-grained, radiate opx -very small branching angles -xals almost appear to be dend	PORPHYRITIC PYROXENE -large, euhedral, sl skel opx with lamellae, settled -75% fine-grained, dendritic and radiate opx	PORPHYRITIC PYROXENE -sub to euhedral, equant, sl skel, settled opx with lamellae -75% coarse, parallel opx dendrites and wheel spoke sph -rounded olivine inclusions in some opx xals

Table 5. CH3 Matrix

	Melt-1500°C/Quench-1200°C	Melt-1487°C/Quench-1187°C	Melt-1475°C/Quench-1175°C	Melt-1450°C/Quench-1150°C
Quench	GLASS	GLASS	PORPHYRITIC PYROXENE -single elong, tab opx -spherulitic quench xtals surround cpx -60% glass	PORPHYRITIC OLIVINE & PYROXENE -skeletal olivine partially enclosed by opx which have lamellae -parallel growth opx dendrites (not perfect extinct.) -fine spherulitic opx
FSO	RADIAL PYROXENE -3 large opx dendrites with nearly parallel arms and slight optical variation across dend -indiv arms skel	GLASS	RADIAL PYROXENE -3 large opx dendrites almost identical to 27 showing some optical variation across dendrite, -arms skel	RADIAL PYROXENE/PORPHYRITIC OLIVINE -opx dendrites with parallel arms which show sl optical mismatch approx 2° -one skeletal olivine xal settled to bottom of charge -minor amts of glass (approx. 5%)
100°/hr	GLASS	PORPHYRITIC PYROXENE -charge contains one (or two?) opx xal which is coarsely dend or skel (If 2 xals - optical mismatch is approx. 3° of rotation)	PORPHYRITIC PYROXENE -subhedral, elong, parallel dend opx -whole charge has 5 xals	PORPHYRITIC PYROXENE -subhedral, elong, sl skel opx,some have lamellae; few, smaller, tab opx -rounded, equant olivine xals settled to bottom, but now incl in opx
5°/hr	PORPHYRITIC OLIVINE -one large, sl skel olivine, bottom of charge -radiating opx with rounded opx throughout -numerous patches of spherulitic opx -sparse glass -silica mineral at outer edge (tridymite)	PORPHYRITIC OLIVINE -one large, highly skel olivine -opx coarsely radiate interspersed with finely spherulitic opx -glass present -silica mineral at outer edge (tridymite?)	PORPHYRITIC PYROXENE -subhedral opx, only cores have lamellae -glass (approx. 10%) which contains opx dendrites -silica mineral at outer edge (tridymite?)	PORPHYRITIC PYROXENE -euhedral, sl skel opx with sparse lamellae -approx. 20% glass -sparse acic opx -outer edge rimmed with SiO₂ mineral (tridymite?) -whole charge has 3 xals

phases nucleate quickly on the crystal remnants present, but beyond a certain point pyroxene grows at the expense of olivine and olivine begins to be resorbed. Aside from anhedral granular masses, pyroxene crystal forms vary from chaotic spherulites and dendrites to highly skeletal and irregular to full equant with decreasing cooling rate.

At $1475^{\circ}C$ only olivine is able to grow during the 17 hour melt. It is found as small rounded crystals, partially settled. With a $65^{\circ}C$/sec. quench these crystals are found in a matrix of glass. At $2500^{\circ}C$/hr. fine exocentraradial pyroxene forms the matrix. At $100^{\circ}C$/hr. cooling run produces large highly skeletal pyroxene crystals with interstitial glass. Minor olivine inclusions are present. At 5°/hr. large skeletal olivine crystals grow surrounded by a mesotasis of accicular to dendritic pyroxene.

At $1500^{\circ}C$ glass is produced in the quench experiment. At a $100^{\circ}C$/hr. cooling rate large highly skeletal pyroxene crystals are produced interstitial glass. Minor olivine inclusions are present. At $5^{\circ}C$/hr. highly skeletal olivine is produced in a mesostasis of olivine dendritic and quench crystals.

Experimental results for CH2 are remarkably similar to those of the PP experiments. Clusters of olivine and pyroxene crystals are present indicating that these are not settled pre-existing crystal remnants in the PP sample but rather early crystallizing phases which cluster together in the early low viscosity liquid.

One subtle difference in texture is the tendency for olivine to form a more barred like texture in the CH2 runs. These are characterized by coarse groups of parallel dendrites. These are not as well developed in the PP runs. This, however, may only be the result of a slight variation in the temperature 'intervals above the liquidus for the respective compositions.

Radial pyroxene samples show similar results to the porphyritic pyroxene samples. The main difference is that radial pyroxene samples show a greater tendency to grow dendritic and coarse radial crystals. Porphyritic olivine samples on the other hand never produce pyroxene. They do however show a complete range in texture from granular to barred.

VI. DISCUSSION

A sequence of crystal forms is evident here. Olivine is found as dendritic, skeletal and equant crystals as well as rounded partially resorbed crystals. Pyroxene varies from fiberous to skeletal dendritic to skeletal equant to complete equant. The progression of crystal form seen here can be explained in terms of heterogeneous nucleation, degree of undercooling and in the case of olivine the presence of a peritectic reaction.

Firstly, the increasing of the melt temperature limits the heterogeneous nuclei available to initiate crystal

growth (Lofgren 1983). This essentially dictates the potential ease of nucleation upon cooling (Gibb, 1974 Fig. 7). This phenomena results in a higher degree of undercooling during cooling. Degree of undercooling is also in part governed by the cooling rate. Faster cooling rate yield a lower critical T (see Fig 8). If cooling rates are faster than equilibrium conditions (as is the case here) a degree of undercooling will be imparted to the liquid. This constitutional undercooling (Lofgren & Donaldson, 1975B; see fig 9) varies directly with cooling rate because diffusion is the limiting process.

In all cases olivine nucleates as the initial phase. This is because it is the liquidus phase and hence has withstood a lesser degree of superheating and secondly because it has a more simple structure it nucleates easily with the presence of heterogeneous nuclei (Kirkpatrick et al.,(1981). Here, however, olivine is a metastable phase and a peritectic reaction takes place to produce pyroxene with further cooling. This reaction is apparently slow in spite of the rapid growth of pyroxene. Under the given cooling conditions the reaction is incomplete and where pyroxene is produced olivine is found as inclusions. With higher melt temperatures the nucleation of pyroxene is inhibied and hence the reaction is inhibited and olivine continues to grow. If pyroxene does finally nucleate the liquid is highly undercooled with respect to pyroxene and highly skeletal dendritic to radial pyroxene forms. If the growth
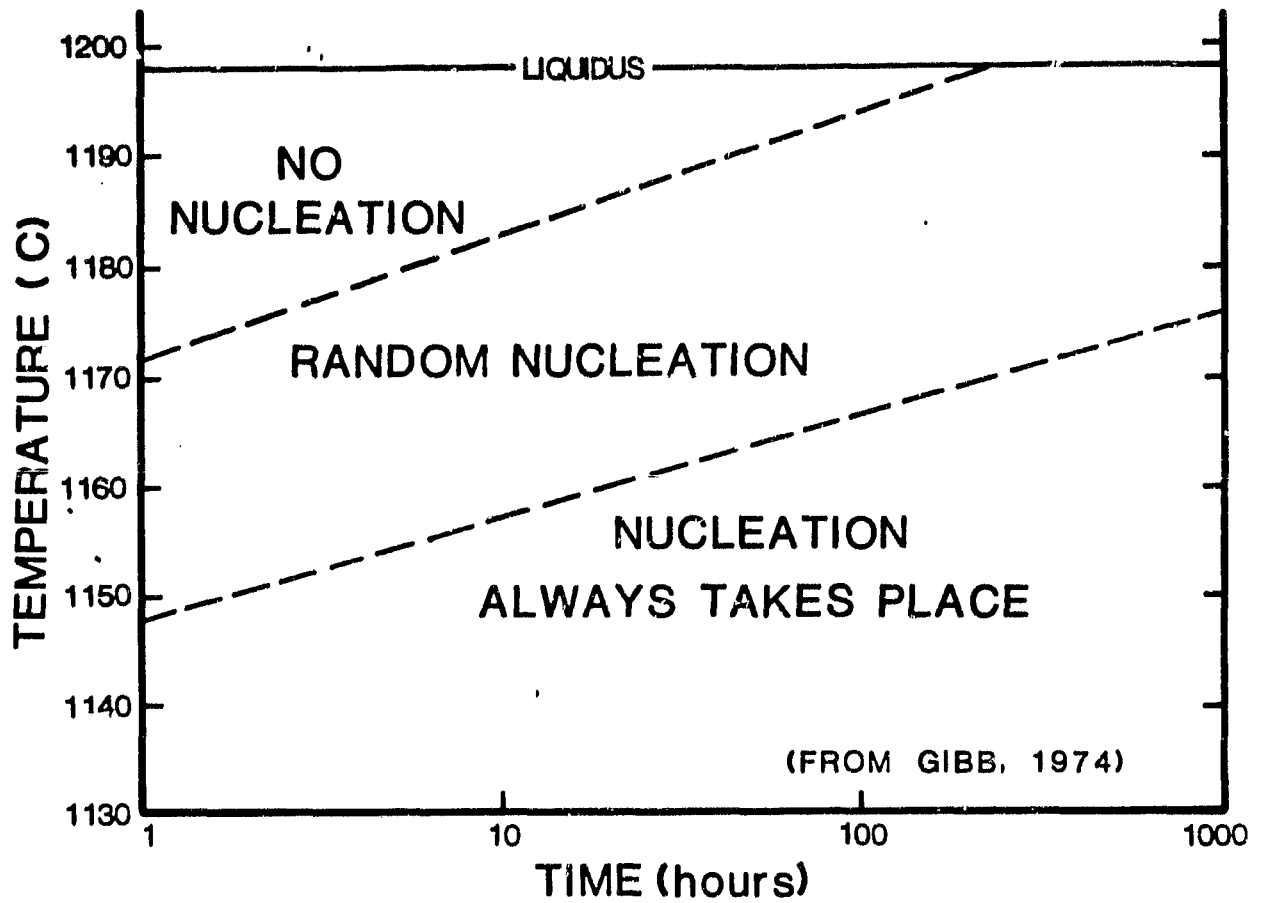
FIG.7 Nucleation behavior of plagioclase from a Columbia Plateau basalt in which plagioclase is the liquidus phase. Principle is the same for olivine and pyroxene in this study.(from Gibb,1974).
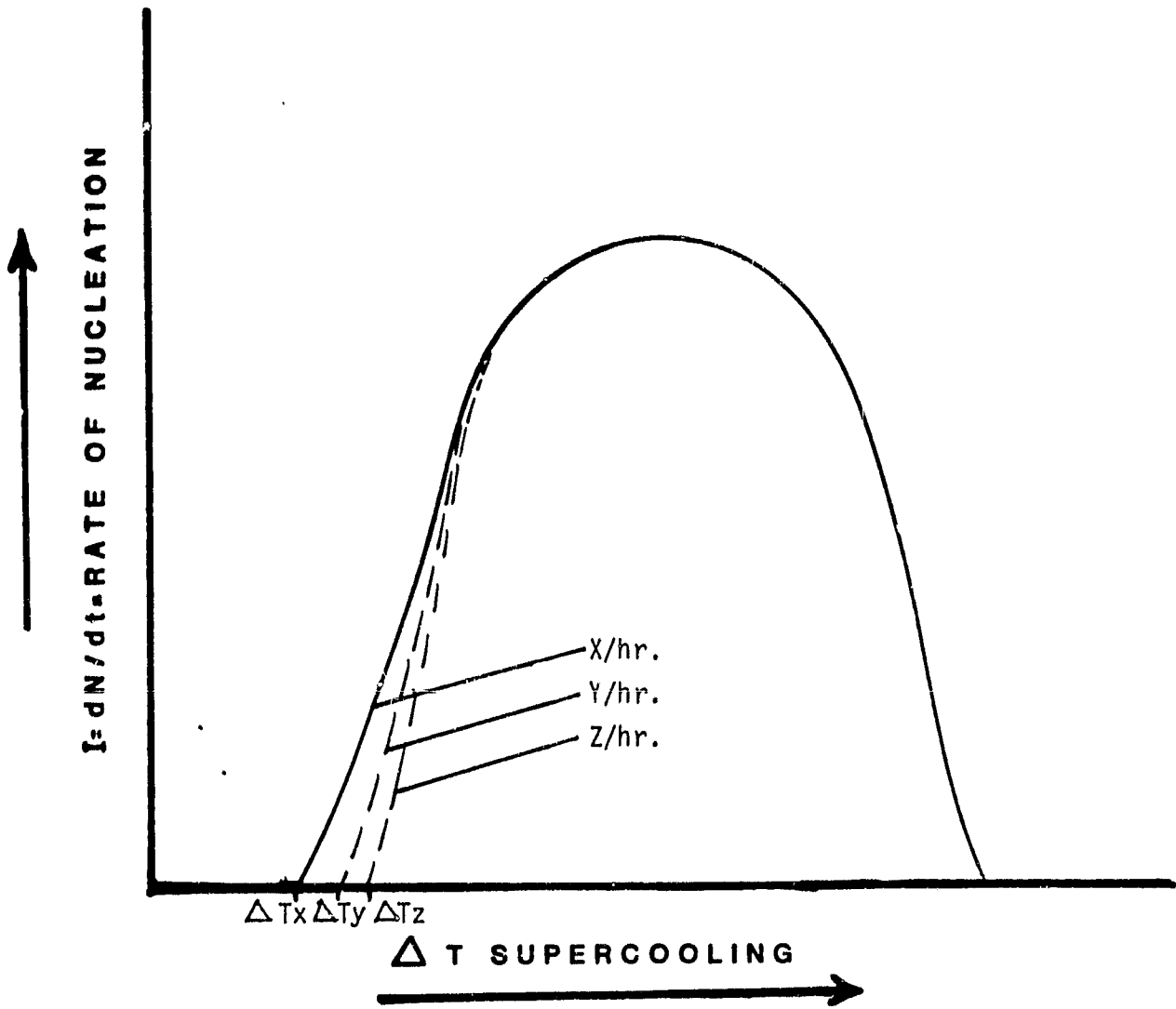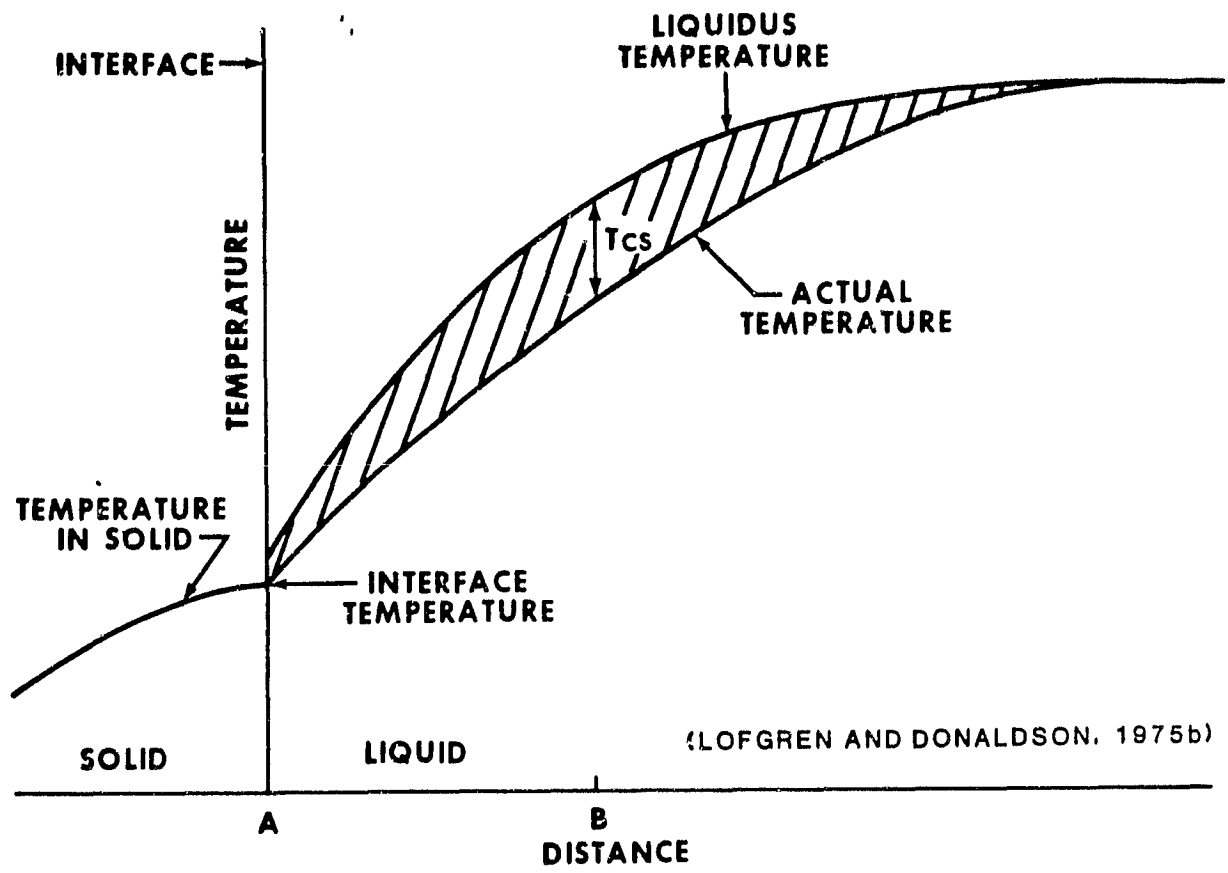
FIG. 8   Schematic representation of effect of cooling
rate on critical T (*$\triangle$T). Note Z   Y   X.

FIG. 9 Schematic representation of constitutional supercooling in advance of a growing crystal interface where the heat is extracted through the crystal. This supercooling exists because low temperature components rejected by the growing crystal do not diffuse away as fast as the crystal inter-face is advancing (from Lofgren, 1980, after Lofgren and Donaldson, 1975b).

of pyroxene is inhibited and the cooling rate is not fast enough to quickly reach the critical T for nucleation of pyroxene then the growth of olivine progresses. This extended growth of olivine can change the co-existing liquid so that it has moved out of or near the edge of the pyroxene crystallization field. This is the case in the super liquidus $5^{\circ}C$/hr. runs. The only pyroxene present is in the form of tiny acicular crystals.

VII. CONCLUSION.

Figure 10 shows a variety of natural chondrules. Comparison with experimental charges (Fig.5and 6) indicates these natural textures have been closely duplicated. Most of these textures can be produced using a single cooling rate with only modest changes in melt temperature. The entire spectrum of textures are produced using some variation in cooling rate coupled with these small variations in melt temperature. We conclude that the melt history is dominant over cooling rate and composition (within the limits of these experiments) in controlling texture. The importance of nuclei, which are most readily derived from pre-existing crystalline material, support an orgin for natural chondrules based on remelting of crystalline material. This would be compatible with a simple, uniform chondrule forming process having only slight variations in thermal histories resulting in the wide range of textures.
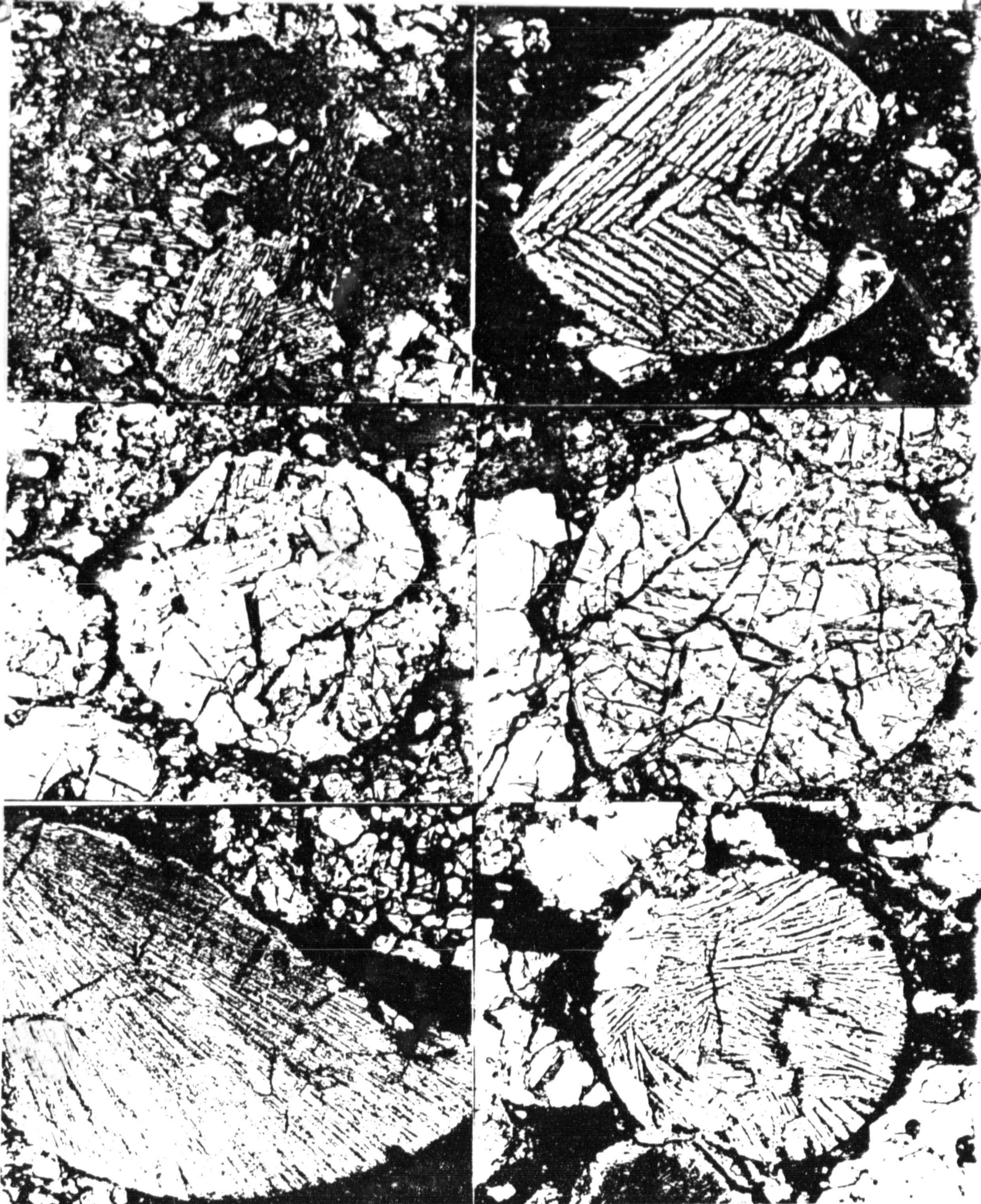
Figure 10. Natural chondrules, A) ALHA-77045,5; B) -79001,7; C) -77249,10
D) -77249,10; E) -77304,29; F) -79001,7.

REFERENCES

Gibb, F.G.F., 1974. Supercooling and the crystallization of plagioclase from a basaltic magma. Miner. Mag. 39, 641-53.

Hewins, R.H., Klein, L.C., and Fasano, B.V., 1981. Conditions of formation of pyroxene excentroradial chondrules. Proc. Lunar Planet. Sci. Conf., 12th, 1123-1130.

Kirkpatrick, R.J., Kuo,L., & Melchior,J., 1981. Crystal growth in incongruently-melting compositions: programmed cooling experiments with diopside.Am. Miner.66,223-41.

Lofgren, G.E., and C.H. Donaldson, 1975b. Curved, branching crystals and differentiation in comb-layered rocks. Contrib. Mineral. Petrol.,49,309-319.

Lofgren, G.E., 1980. Experimental studies on the dynamic crystallization of silicate melts. In: Hargraves, R.B. (ed.) Physics of Magnetic Processes. Princeton Univ. Press, 487-551.

Lofgren, G.E., 1983. Effect of heterogeneous nucleation on basaltic textures: a dynamic crystallization study. Jour. of Petrol., 24, 229-255.

Lofgren, G.E., Russell, W.J., and Kinnebrew, Q., 1983. Dynamic crystallization experiments on chondrule melts of porphyritic pyroxene composition. Abstr. Lunar Sci. Conf. 15th, 489-90.

Lofgren, G.E., Kinnebrew, Q., and Russell, W.J., 1983. Dynamic crystallization experiments on chondrule melts of radial pyroxene composition. Abstr. Lunar Sci. Conf. 487-488.

Nafziger, R.H., Ulmer, G.C., and Woermann, Ed, 1971. Gaseous buffering for the control of oxygen fugacity at one atmosphere. Research Techniques for High Pressure and Temperature, Gene C. Ulmer, ed., Springer Verlag (New York), 9-41.

Tsuchiyama, A., Nagahara, H., and Kushiro, I., 1980. Investigations on the experimentally produced chondrules: Chemical compositions of olivine and glass and formation of radial pyroxene chondrules. Memoirs of National Institute of Polar Research Special Issue, 20, 83-94.

Tsuchiyama, A., Nagahara, H., and Kushiro,I., 1980. Experimental reproduction of textures of chondrules. Earth and Planetary Science Letters, 48, 155-165.

Tsuchiyama,A., and Nagahara, H., 1981. Effect of precooling
history and cooling rate on the texture of chondrules:
preliminary report. Memoirs of National Institute of
Polar Research Special Issue, 20, 175-192.

Williams, R.J., and Mullins, O.Jr., 1981. JSC systems using
solid ceramic oxygen electrode cells to measure oxygen
fugacities in gas-mixing furnaces. NASA TMX-58234.
Houston.